Sigma J Eng Nat Sci, Vol. 44, No. 1, pp. 273–291, February, 2026

Sigma Journal of Engineering and Natural Sciences
Web page info: https://sigma.yildiz.edu.tr
DOI: 10.14744/sigma.2026.1982

Research Article

Image segmentation for semi-supervised fuzzy clustering with KL-divergence using Kernel method

Muthulakshmi K, Jayalakshmi M*

[1]*Department of Mathematics, Vellore Institute of Technology, Vellore, Tamil Nadu, 632014, India*

ARTICLE INFO

Article history
Received: 10 September 2024
Revised: 17 October 2024
Accepted: 08 December 2024

Keywords:
Fuzzy Cluster; Kernel Distance Measures; Robustness; Semi-Supervised; Uncertainty

ABSTRACT

Image segmentation is computer vision and analysis of images. However, several segmentations couldn't be manageable due to high noise levels. It is tough to deal with semi-supervised fuzzy clustering since it is not robust, and reduction needs to be improved. Many researchers have developed in this cluster. Our research focuses on adding noise, reducing noise, and applying our techniques to get detailed, clear images. Now, we introduce the robust approach kernel method based on semi-supervised fuzzy clustering with Kullback-Leibler divergence. It incorporates Kullback-Leibler divergence, and semi-supervised clustering is of essential significance. The primary benefit of robust semi-supervised fuzzy clustering is that it manages uncertainty data and kernel distance measures to capture the similarity between data points, enhancing segmentation performance. We use various strategies to introduce noise and minimise it compared to kernel robustness semi-supervised fuzzy clustering with Kullback-Leibler divergence. The effectiveness of the recommended technique was evaluated using synthetic datasets, the publicly accessible simulated human brain Magnetic Resonance Imaging dataset, and the BraTS2020 medical imaging and lung computed tomography scans. The experimental findings show that the suggested method outperforms existing algorithms in peak signal noise ratio, accuracy, precision, F1 score, and Jaccard index.

Cite this article as: K M, M J. Image segmentation for semi-supervised fuzzy clustering with KL-divergence using Kernel method. Sigma J Eng Nat Sci 2026;44(1):273–291.

INTRODUCTION

Image segmentation is the most essential need; day by day, they can quickly analyse something early. However, traditional approaches often break down when dealing with complex images with a lot of noise. The noise reduction achieved by traditional fuzzy clustering approaches needs to improve due to their lack of robustness. Because it produces precise images without ionising radiation, Magnetic Resonance Imaging (MRI) is crucial to modern medicine and ensures patient safety. Because MRI can produce multidimensional, high-contrast images, it is beneficial in the research of more delicate brain regions, such as the white matter (WM), grey matter (GM), and cerebrospinal fluid (CSF). It is essential for target detection and pattern recognition tasks in medical image processing. Many segmentation algorithms have developed, such as spectral clustering

***Corresponding author.**
*E-mail address: m.jayalakshmi@vit.ac.in

This paper was recommended for publication in revised form by Editor-in-Chief Ahmet Selim Dalkilic

approaches [1], density clustering [2], threshold-based methods [3], and level set methods [4].

With a large amount of MRI data generated daily, faster and more accurate analysis of this data is desired, which requires skilled radiologists. However, radiologists manually analyse these images, which is time-consuming. Further, the varying knowledge level of radiologists makes analysing these images inconsistent. All these factors require automated algorithms to support radiologists in providing quicker and more efficient analysis of these images. Supervised learning is completely labeled data. Unsupervised learning is completely unlabeled samples [5]. It is used for assigning data points to clusters when there is no available information about the correct clustering. Semi-supervised and unsupervised learning are more favorable than supervised learning since they are time-consuming and most practical real-world situations do not require previous knowledge. In this literature introduces many automated medical image segmentation methodologies, including clustering algorithms. Clustering belongs to the class of unsupervised learning methods in which there is no given information about the labels of the data elements, dissimilar to classification methods. It is most successful because it provides a decent trade-off between time complexity and segmentation quality, a key shortcoming of most other approaches. One of the popular techniques is fuzzy set theory, especially in medical image segmentation, because of the inherent ambiguity of images and the complexity of human vision. Fuzzy theory and clustering technologies have generated a lot of academic interest. Deep learning is frequently used to assess comparable performance indicators like accuracy (Acc), precision (Pre), recall (RC), and F1 scores have been evaluated [6]. Many clustering algorithms are available in the literature, broadly categorised into hard clustering [7] and soft clustering [8,9] strategies. Methods like kernel-based algorithms [10], SVM [11], and K-means clustering have garnered significant attention, leading to several extensions such as fuzzy ISODATA [1], kernel principal component analysis, KFDA [12], neutrosophic set [13], kernel-based algorithms, and Grey Wolf Optimizer [14]. RBF networks [1] using segment regions of clusters have shown to be particularly advantageous and may have been applied to overcome issues in numerous communication systems.

Bezdek et al. created the fuzzy c-means (FCM) clustering, a soft clustering method inspired by Zadeh's fuzzy set theory [15,16]. Pixels can be assigned to many clusters at once by changing their degree of membership. FCM is a center-based clustering algorithm that modifies the degree of membership inversely based on a pixel's distance from the cluster centers [17,18]. Many researchers have been attempting to improve the FCM algorithm for medical image segmentation, addressing difficulties including low sharpness and poor understanding, which need clarification. However, research has found problems with FCM-based clustering algorithms due to reluctance when allocating membership functions. As a result, several researchers have developed the intuitionistic fuzzy c-means (IFCM) based on an intuitionistic fuzzy set (IFS) expanded by Atanassov [19], which considers membership, non-membership and hesitation degrees, hence enhancing clustering outcomes for imprecise data. FCM uses Euclidean distance in the original feature space, making it a less noisy environment, whereas kernel-based fuzzy clustering transforms data into a higher-dimensional space, improving cluster [20]. Lavanya [21] developed the modified quick kernel-induced intuitionistic fuzzy generator to enhance input images by minimising uncertainty. The grey-level histogram of the morphologically reconstructed IFS picture is subsequently examined utilising the kernel distance of IFCM clustering [14]. Additionally, Bui Cong Cuong [22] published image fuzzy sets in 2014, paving the way for the development of picture fuzzy clustering (PFCM) for tumor segmentation, which accounts for degrees of rejection, membership, neutrality, and non-membership. Chengmao Wu [23] enhanced the robustness of prior PFCM algorithms by resolving issues related to the selection of spatial constraint parameters, leading to the development of a novel PFCM, the resilient dynamic semi-supervised symmetric regularised PFCM [24], which incorporates Kullback-Leibler (KL) divergence [25] and spatial information prerequisites. Inder Khatri also kernel fuzzy clustering, which can explore non-linear relations of pixels in an image [26]; its basic idea is to implicitly transform the input data into a higher dimensional feature space via a nonlinear map, which greatly increases the possibility of linear separability of the patterns in the feature space, then perform FCM in the feature space, which enhances boundary detection and adapts to complex shapes [9]. This method calculates fuzzy memberships with greater precision, mitigating boundary leakage and enhancing contour accuracy despite noise, as an extension of image fuzzy set-based clustering techniques that employ picture fuzzy sets and the KL divergence metric. In 2015, R. R. Gharieb [26] proposed a method for integrating local membership data into conventional FCM clustering via regularisation using KL divergence. Kamil Kmita [12] developed a scaling factor α that affects partial supervision as a nonlinear function in fuzzy clustering. Then developed semi-supervised clustering improves unsupervised clustering algorithms, and labeled data is highly scarce. Acquiring labeled samples is difficult and laborious. The labelling of all data is a labour-intensive endeavour because to the substantial volume of real-world data and the rapid pace of data generation, particularly in a streaming data context. Semi-supervised fuzzy clustering analysis of scaling factor descriptions validate their similarity and corroborate the interpretation by Pedrycz and Waletzky [9]. Kernel-based semi-supervised clustering [27] has been proposed and applied in many fields. According to the scaling factor, optimization requires balancing supervised and unsupervised components, which results in improved image feature interpretation and the ability to do further clustering. It improves the algorithm using KL-divergence, which helps maintain the two-probability distribution. It also helps

measure spatial data distribution, ensuring that the clustering process remains sensitive to noise and uncertainty while preserving the structure of the segmented regions. In my research case, modifying the algorithm improves the clustering accuracy. It has been successfully used in classification and clustering problems. Morphological reconstruction has been smoothing out excess connected pixels while retaining contour information to understand the clustering process better. It addresses the problem of balancing the number of segmented regions with the contour accuracy. Clustering methods are applied after the image's grey-level histogram to save processing time. Finally, the Gaussian kernel distance measure is utilized to compute the distance measure in higher dimensional feature space. Due to the transformation of data points in higher dimensional feature space, the Gaussian kernel can solve the problem of inherent non-linearity in data without increasing the computational complexity. We incorporate this method by implementing Kernel based on semi-supervised fuzzy clustering with KL-divergence (KSSFKL) on the histogram of morphologically rebuilt images and a unique FCM that clusters complicated data without hesitation and in less time, which gives a better tradeoff between robustness to noise and shape preservation.

In summary of major contribution:

1. The clustering optimization problem is formulated within a semi-supervised theoretical framework, effectively addressing noise and non-linearity. A unique semi-supervised FCM method is being developed to improve cluster representation capabilities and decision-making.
2. The proposed method reduces noise in segmentation by incorporating KL divergence metrics. In addition, kernel distance aims to handle non-linear systems effectively.
3. As a result, the proposed clustering approach mitigates noise and non-linear structures found in images and substantially enhances segmentation tasks, providing a promising prospect for future applications.

The remainder of the article is structured into five sections, each building upon the previous one. Section 2 delineates the preparatory measures necessary for the proposed methodology, establishing the foundation for our research. Section 3 comprehensively elucidates the clustering process, which constitutes the essence of our methodology. Section 4 subsequently concentrates on parameter selection and experimental analysis, utilising the techniques from preceding parts. Section 5 presents and elucidates the calculated results derived from our experimental endeavours. Finally, sections 6 and 7 discuss the suggested technique and the conclusion of our study.

PRELIMINARIES

This section comprises definitions and explanations of the fundamental concepts utilized in this study. It delineates the fundamental principles and approaches utilised, together with the corresponding notations employed throughout the work.

Fuzzy C-means Clustering

The incorporation of fuzzy logic into the FCM technique represents an extension of the widely-used K-means algorithm for clustering. The FCM algorithm, like K-means, is iterative, with a preset beginning grouping and several clusters (C). Let $T = (y_1, y_2, \ldots, y_N)$ denote the collection of data points, and $V = \{v_1, v_2, \ldots, v_C\}$ represent the center of cluster. FCM algorithm aims to minimize the following objective function to divide N data points into C clusters.

$$J = \sum_{j=1}^{N}\sum_{i=1}^{C} u_{ij}^{m} \left\|y_j - v_i\right\|^2, \quad 1 < m < \infty, \tag{1}$$

The fuzzy partition matrix $U = (u_{ij})_{C*N}$ meets the following conditions, with m representing the weighting exponent:

$$u_{ij} \in [0,1], \quad \sum_{i=1}^{C} u_{ij} = 1, 1 \le i \le C, 1 \le j \le N \tag{2}$$

where the value of membership u_{ij} for the j^{th} pixel in the i^{th} cluster, denoted by v_i, is determined by the square Euclidean distance $\|y_j - v_i\|^2$. Here, $m \in [1,\infty]$ is an integer that regulates the fuzziness exponent. The membership degree u_{ij} and the cluster center v_i can be expressed using the Lagrange multiplier method as follows:

$$u_{ij} = \frac{\left(\left\|y_j - v_i\right\|^2\right)^{\frac{-1}{m-1}}}{\sum_{k=1}^{C}\left(\left\|y_j - v_k\right\|^2\right)^{\frac{-1}{m-1}}} \tag{3}$$

$$v_i = \frac{\sum_{j=1}^{N} u_{ij}^{m}\, y_j}{\sum_{j=1}^{N} u_{ij}^{m}}, \quad 1 \le i \le C \tag{4}$$

Semi-supervised Clustering

Traditional fuzzy clustering methods treat pixels independently, which is not optimal for pixel clustering. Pedrycz et al. [12] proposed an SSFCM to improve FCM clustering performance. The optimization models for the SSFCM algorithm are delineated as follows [24]:

$$\begin{aligned} J = &\sum_{j=1}^{N}\sum_{i=1}^{C} u_{ij}^{m} \left\|y_j - v_i\right\|^2 \\ &+ \rho \sum_{j=1}^{N}\sum_{i=1}^{C} \left(u_{ij} - f_{ij} b_i\right)^m \left\|y_j - v_i\right\|^2 \end{aligned} \tag{5}$$

where $\sum_{j=1}^{N} u_{ij}, i = 1, 2, \ldots, N$. Ref. [1] provides a detailed description of the parameters ρ, b_i, and supervised information f_{ij}. The membership degree u_{ij} and cluster center v_i can be expressed as follows.

$$u_{ij} = \frac{1}{1+\rho}\left[\frac{1+\rho\left(1-b_i\sum_{k=1}^{C} f_{ij}\right)}{\sum_{k=1}^{C}\frac{\|y_j - v_i\|^2}{\|y_j - v_k\|^2} + \rho f_{ij} b_i}\right] \quad (6)$$

$$v_i = \frac{\sum_{j=1}^{N} u_{ij}^m y_j + \rho\sum_{j=1}^{N}\left(u_{ij} - f_{ij}b_i\right)^2 y_j}{\sum_{j=1}^{N} u_{ij}^m + \rho\sum_{j=1}^{N}\left(u_{ij} - f_{ij}b_i\right)^2} \quad (7)$$

If $\rho = 0$, the SSFCM method transforms into the standard FCM algorithm. Thus, the FCM algorithm is an upgraded version of the SSFCM technique.

Fuzzy c means with KL-Divergence

In Ref. [14], the FCM algorithm's objective function updates a regularisation technique that includes an entropy term. This approach [24] is defined as:

$$J = \sum_{j=1}^{N}\sum_{i=1}^{C} u_{ij}^m \|y_j - v_i\|^2 + \lambda\sum_{j=1}^{N} u_{ij}\log\frac{u_{ij}}{\pi_{ij}} \quad (8)$$

Where π_{ij} is represented as the average local membership function.

$$\pi_j = \frac{1}{N_k}\sum_{j=1}^{N} u_{ij}$$

As a result, the KL divergence [26] is minimized, guiding u_{ij} towards the membership value, and the average pixel π_{ij} consider as an adjacent neighbourhood. This strategy produces piecewise homogenous labeling and can be used to smooth noise. The equation (8) is minimized by:

$$u_{ij} = \frac{\pi_j \exp\left(-\frac{\|y_j - v_i\|^2}{\lambda}\right)}{\sum_{k=1}^{C}\pi_k \exp\left(-\frac{\|y_j - v_k\|^2}{\lambda}\right)} \quad (9)$$

$$v_i = \frac{\sum_{j=1}^{N} u_{ij}^m\, y_j}{\sum_{j=1}^{N} u_{ij}^m}, \quad 1 \le i \le C \quad (10)$$

PFCM

Cuong [22] developed the Picture Fuzzy Set (PFS) concept, which extends the traditional fuzzy set and IFS. A PFS defined on a non-empty set *X* and a positive degree in FCM represents the probability that a sample belongs to a particular cluster. As a result, the literature proposes a novel PFS with a clustering approach [28], with an optimization model described as:

$$J = \sum_{j=1}^{N}\sum_{i=1}^{C}\left(\frac{u_{ij}}{1-\zeta_{ij}-\varrho_{ij}}\right)^m \|y_j - v_i\|^2 \quad (11)$$

The following conditions are satisfied by the constraints:

$$0 \le u_{ij}, \zeta_{ij}, \varrho_{ij} \le 1, 0 \le u_{ij} + \zeta_{ij} + \varrho_{ij} \le 1, , i = 1,2,\dots,N.$$

$$\sum_{j=1}^{N}\left(\frac{u_{ij}}{1-\zeta_{ij}-\varrho_{ij}}\right)^m = 1\ , i = 1,2,\dots.,N$$

$$\sum_{j=1}^{N}\left(\zeta_{ij} + \varrho_{ij}/C\right) = 1\ , i = 1,2,\dots.,N.$$

Which as *N*, *C*, y_j and v_i represent the no. of samples, the no. of clusters, the i^{th} sample in the dataset y_j, and the center of cluster of the j^{th} cluster, respectively. Additionally, u_{ij}, ζ_{ij} and ϱ_{ij} denote the positive, neutral, and refusal degree of sample y_j belongs to the i^{th} cluster.

$$u_{ij} = \frac{1-\zeta_{ij}-\varrho_{ij}}{\sum_{k=1}^{C}\left(\frac{\|y_j - v_i\|^2}{\|y_j - v_k\|^2}\right)^{\frac{1}{m-1}}} \quad (12)$$

$$v_i = \frac{\sum_{j=1}^{N}\left(\frac{u_{ij}}{1-\zeta_{ij}-\varrho_{ij}}\right)^m y_j}{\sum_{j=1}^{N}\left(\frac{u_{ij}}{1-\zeta_{ij}-\varrho_{ij}}\right)^m} \quad (13)$$

$$\zeta_{ij} = 1 - \varrho_{ij} - \frac{\frac{C-1}{C}}{\sum_{k=1}^{C}\frac{u_{ij}}{u_{ik}}\left(-\frac{\|y_j - v_i\|^2}{\|y_j - v_k\|^2}\right)^{\frac{1}{m-1}}} \quad (14)$$

$$\varrho_{ij} = 1 - \left(u_{ij} + \zeta_{ij}\right) - \left(1 - \left(u_{ij} + \zeta_{ij}\right)^{\alpha}\right)^{\frac{1}{\alpha}} \quad (15)$$

Kernel Method

Kernel-based machine learning techniques, such as SVM [29], Kernel Principal Component Analysis (KPCA) [11], and Kernel Fisher Discriminant (KFD) [30], have demonstrated efficiency in various classification and feature extraction tasks. The based-on-kernel approach facilitates [21] the feature mapping space from its original dimensionality to a kernel equation, transforming a higher-dimensional space and allowing for arbitrary nonlinearity. This characteristic enhances the linear machine's expressiveness, and its integration into clustering algorithms can improve their clustering power and accuracy. The main advantage of

kernel methods lies in the fact that the dot product in the kernel space is such that,

$$K(y_i, y_j) = \phi(y_i)^T \phi(y_j) \tag{16}$$

where y_i represents the data in the original space while $\phi(y_j)$ represent as the data in higher-dimensional space. Kernel equations that are frequently employed [24] include there are four kernel functions: linear, polynomial of degree p, Sigmoid and Gaussian radial basis function [31] (RBF). These are provided as follows:

$$\begin{aligned} K(y_i, y_j) &= y_j^T y_i \\ K(y_i, y_j) &= \left(1 + y_j^T y_i\right)^p \\ K(y_i, y_j) &= \tanh\left(\rho\left(y_j^T y_i\right) + \beta\right) \\ K(y_i, y_j) &= exp\left(-\frac{\left\|y_i - y_j\right\|^2}{\sigma^2}\right) \end{aligned}$$

Equation (16) allows the preceding equation to be represented as:

$$\begin{aligned} \left\|\phi(y_i) - \phi(y_j)\right\|^2 = K(y_i, y_i) + K(y_j, y_j) \\ - 2K(y_i, y_j) \end{aligned} \tag{17}$$

The Gaussian RBF kernel can be represented as:

$$\left\|\phi(y_i) - \phi(y_j)\right\|^2 = 2\left(1 - K(y_i, y_j)\right) \tag{18}$$

Similarly, the Euclidean distance between extra kernel spaces by applying a suitable kernel function in equation (17).

Kernel-based on picture fuzzy clustering with KL-divergence

Optimize PFS using kernel fuzzy clustering and KL-divergence metric, as described in [32-35].

$$\begin{aligned} J = &\sum_{j=1}^{N}\sum_{i=1}^{C}\left(u_{ij}(2 - \varrho_{ij})\right)\left(1 - k(y_j, v_i)\right) \\ &+ \gamma\sum_{j=1}^{N}\sum_{i=1}^{C} u_{ij}\left(2 - \varrho_{ij}\right)\log\frac{u_{ij}(2 - \varrho_{ij})}{\pi_{ij}} \\ &+ \sum_{j=1}^{N}\sum_{i=1}^{C}\left(\zeta_{ij}(\log\zeta_{ij} + \varrho_{ij})\right) \end{aligned} \tag{19}$$

Where $\pi_{ij} = \frac{1}{N}\sum_{j=1}^{N} u_{ij}(2 - \varrho_{ij})$

The following satisfied constraints:

$$\begin{aligned} &0 \le u_{ij}, \zeta_{ij}, \varrho_{ij} \le 1, \\ &0 \le u_{ij} + \zeta_{ij} + \varrho_{ij} \le 1, 1 \le i \le C, 1 \le j \le N \\ &\sum_{i=1}^{C} u_{ij}\left(2 - \varrho_{ij}\right) = 1, 1 \le j \le N \\ &\sum_{i=1}^{C}\left(\zeta_{ij} + \varrho_{ij}/C\right) = 1, 1 \le j \le N, \end{aligned}$$

Where $k(y_j, v_i) = \exp\left(-\frac{\left\|y_j - v_i\right\|^2}{\sigma^2}\right)$ is defined by kernel distance measure and where γ is the regularization parameter. Here, v_i for all $i = 1, 2, ..., C$ and $j = 1, 2, ..., N$, y_j represents the cluster centers and data point centroids. After solving the equation (19) is an optimization problem, the degree of membership values u_{ij}, center of cluster v_i, neutrality degree ζ_{ij}, and refusal degree ϱ_{ij} may be Langrage's indetermined multipliers method derived from the following condition:

$$u_{ij} = \frac{\pi_{ij}\exp\left(\frac{-\left(1 - y_j - v_i\right)}{\gamma}\right)}{\sum_{l=1}^{C}\pi_{lj}\exp\left(\frac{-\left(1 - y_j - v_i\right)}{\gamma}\right)}\frac{1}{\left(2 - \varrho_{ij}\right)} \tag{20}$$

$$v_i = \frac{\sum_{j=1}^{N}\left(u_{ij}\left(2 - \varrho_{ij}\right)\right)\left(k(y_j, v_i)\right)y_j}{\sum_{j=1}^{N}\left(u_{ij}\left(2 - \varrho_{ij}\right)\right)\left(k(y_j, v_i)\right)} \tag{21}$$

$$\zeta_{ij} = \frac{\exp\left(-\varrho_{ij}\right)}{\sum_{l=1}^{C}\exp\left(-\varrho_{ij}\right)}\left(1 - \sum_{l=1}^{C}\frac{\varrho_{lj}}{C}\right) \tag{22}$$

$$\varrho_{ij} = 1 - \left(u_{ij} + \zeta_{ij}\right) - \left(1 - \left(u_{ij} + \zeta_{ij}\right)^{\alpha}\right)^{\frac{1}{\alpha}} \tag{23}$$

MATERIALS AND METHODS

As previously mentioned, non-linear features and image noise present significant challenges for image segmentation. In this literature has proposed various fuzzy set theory-based techniques to address these difficulties. The main objective of this correct selection of regularization parameter values substantially impacts segmentation performance in noisy pictures. Figure 1 displays the main framework of the proposed approach.

Image segmentation in noisy and uncertain environments, especially medical images, poses significant challenges. This research presents a semi-supervised clustering strategy for image segmentation. It is one of the techniques that addresses the challenges of improving clustering accuracy under the supervision of a limited amount of data. In this case, the optimization using robust kernel-based semi-supervised fuzzy clustering optimization problem using the KL-divergence. This optimization issue consists of three words that attempt to overcome the constraints of present approaches. The first term uses kernel distance metrics to deal with non-Euclidean distance. The second term attempts to reduce noise during segmentation by using the KL divergence metric, adding neighbourhood information to assign pixel cluster labels appropriately by introducing model fuzziness. The third term improves clustering quality by minimizing the information required for

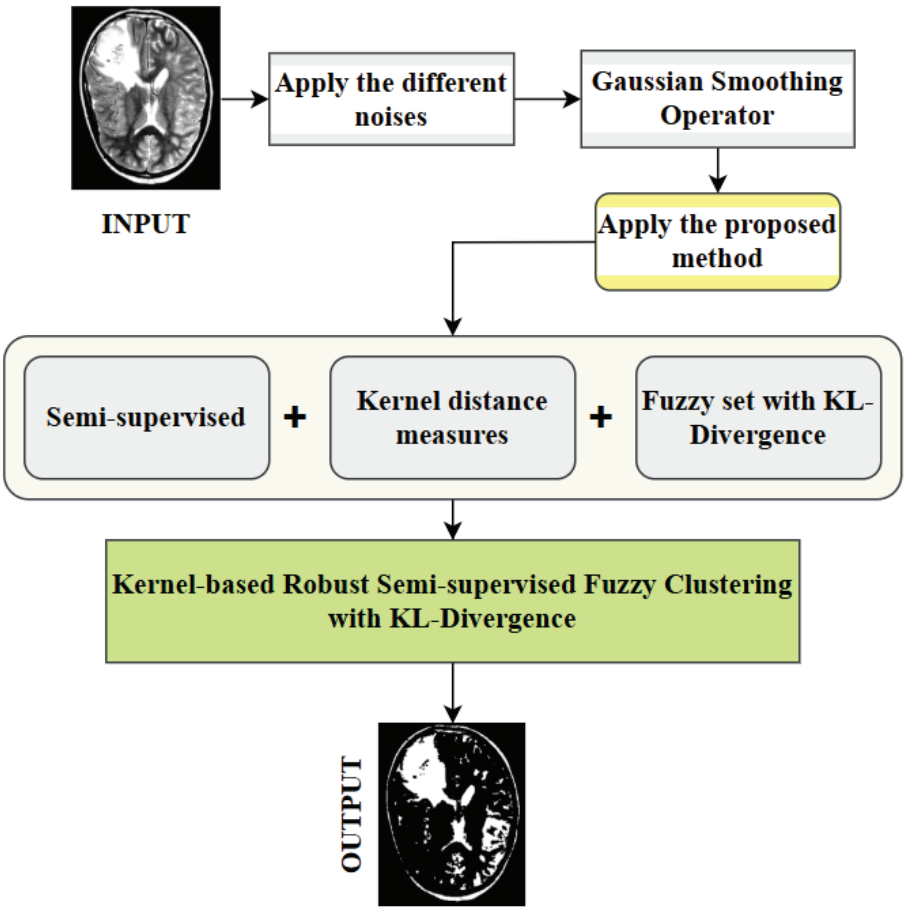

Figure 1. Flow chart of the proposed work

semi-supervised algorithms to acquire optimal cluster locations. This approach is defined as:

$$J = \sum_{j=1}^{N}\sum_{i=1}^{C} u_{ij}^{m}\left(1 - k(y_j, v_i)\right) + \rho \sum_{j=1}^{N}\sum_{i=1}^{C}\left(u_{ij} - f_{ij}b_i\right)^{m}\left(1 - k(y_j, v_i)\right) + \lambda \sum_{j=1}^{N}\sum_{i=1}^{C}\left(u_{ij}(\log u_{ij})\right) \quad (24)$$

$\rho \geq 0$ is a scaling factor that controls the ratio of supervised and unsupervised components in the optimization method. We employ a two-value boolean indicator $b = [b_k]$, with $k = 1, 2, ..., N$ with either 0 or 1 entries to discriminate between labeled and unlabeled structures. Similarly, $F = [f_{ik}]$ is the labeled patterns of the membership function recognized in matrix form, denoted as where $i = 1, 2, ..., C$, $K = 1, 2, ..., N$. Using the kernel distance metric, we use Gaussian representations for cluster centroids and data points. It deals with the non-linear structure present in data. Due to the transformation of data points in higher dimensional feature space, the kernel trick can solve the problem of inherent non-linearity present in data without increasing the computational complexity. After addressing the optimization issue, the value of membership function u_{ij} and center of cluster v_i and using calculating Lagrange's approach using indeterminate multipliers, as follows:

$$u_{ij} = \frac{\exp\left(\frac{-\lambda + 2(1+\rho)\left(1 - k(y_j, v_i)\right)\left[\rho\sum_{i=1}^{c} f_{ij}b_j - u_{ij}\right]}{\lambda}\right)}{\sum_{k=1}^{c}\exp\left(\frac{-\lambda + 2(1+\rho)\left(1 - k(y_j, v_k)\right)\left[\rho\sum_{i=1}^{c} f_{ij}b_j - u_{ij}\right]}{\lambda}\right)} \quad (25)$$

$$v_i = \frac{\sum_{j=1}^{N} u_{ij}k(y_j, v_i)y_j + \rho\sum_{j=1}^{N}\left(u_{ij} - f_{ij}b_i\right)^2 y_j}{\sum_{j=1}^{N} u_{ij}k(y_j, v_i)y_j + \rho\sum_{j=1}^{N}\left(u_{ij} - f_{ij}b_i\right)^2} \quad (26)$$

The primary purpose of this strategy is to reduce the weighted sum of squared distances between data points and their cluster centers while also integrating robust constraints and a regularisation term to encourage smooth cluster memberships. This iterative approach is intended to reduce the effect of noise and properly locate cluster

centers in noisy image environments (Appendix A). These are ensured that the following steps improves the clustering and decision-making is more reliable, even when faced with noise and uncertainty (Algorithm 1).

Algorithm 1. KKSFKL Algorithm
1: Step 1: Given the number of clusters C, parameters b and f choose the distance function and initialize the partition matrix including membership values.
2: Step 2: Calculate the cluster centers v_i using equation 26 and the distances between data points and cluster centers.
3: Step 3: Update the membership values u_{ij} in accordance with equation 25.
4: Step 4: If U - $U' < \delta$ then
5: Stop
6: Else
7: Set $U = U'$ and go to Step 2

Advantage
- ✓ The proposed semi-supervised clustering approach produces strong segmentation results by reducing the effects of noise and nonlinearity.
- ✓ Using KL-divergence together with kernel-based distance measures improves cluster descriptions and supports reliable segmentation, even under challenging conditions.

Disadvantage
- ✓ Our performance in achieving segmentation results is generally good, but we struggle with maintaining accuracy in the presence of noise.

PARAMETER SELECTION

In order to validate the efficacy of the proposed KSSFKL method, we have performed experiments on five open-access and synthetic datasets, two open brain tumor datasets and a computed tomography (CT) scan image. The experiment aims to show the effectiveness of the proposed KSSFKL clustering approach for image segmentation tasks for different kinds of images, including natural and medical images. Experiments are designed to check the proposed method's efficacy compared to other related methods such as FCM, FCMKL, PFCM, and KFPKL. The list of parameters is presented in Table 1. Quantitative and qualitative results are obtained on several images for comparison purposes. Evaluating PSNR, Acc, Pre, F1, and JI are used to measure the segmentation quality by comparing the predicted clusters against GT, mainly focusing on boundary accuracy and region overlap. They are used as quantitative measurements to assess the resilience of different clustering from segmentation approaches against noise. These metrics thoroughly assess the method's proficiency in precisely segmenting regions of interest while reducing noise and border inaccuracies. PSNR measures the image quality after segmentation, while accuracy, Jaccard index, and Dice coefficient evaluate how well the segmented regions match the GT. This research evaluates the algorithm's efficiency, which is described as several types of noise, and introduces it to different grayscale images for segmentation tests in Python. FCM, FCMKL, PFCM, KFPKL, and KSSFKL are suggested algorithms used in segmentation testing. PSNR, Acc, Pre, F1, and JI are used as quantitative measurements to assess the resilience of different clustering from segmentation approaches against noise. $\in = 0.0001$ is the iteration error, and then the maximum iteration is $t_{max} = 1000$.The statement KSSFKL gives better results compared to other algorithms implies that in experimental or empirical evaluations, KSSFKL in this performance metric is greater than the other performance.

Table 1. List of parameter values associated with each method

Method	Input Parameters & Value
FCM	m = 2, n = 5
FCMKL	m = 2, n = 4, λ = 1.0, h = 0.1
PFCMPFCM	m = 2, n = 5, α = 10
KFPKL	m = 3, n = 2, α = 1, γ = 1, σ = 10
KSSFKL	m = 2, n = 2, α = 10, λ = 10, σ = 70

Evaluations

To compare the performance of several clustering techniques honestly using segmentation, the improved peak signal noise ratio (PSNR) is used as a crucial assessment metric and to analyze the suggested algorithm's resilience to noise. The improved PSNR is as follows:

$$PSNR = 10log_{10}\left(\frac{255^2}{\text{MSE}}\right)$$

Here, mean square error (MSE) [20] measures the discrepancy between the segmentation results and the GT image achieved by the method. A higher PSNR value indicates the method's robustness against noise and provides reassurance that the model is less sensitive to noise during the segmentation process.

Furthermore, to completely evaluate the proposed algorithm's segmentation and clustering performance, we must use [24] pixel Acc, Pre, F1, and JI as metrics. These measures are described as follows:

The ratio of correctly identified total number of samples is used to calculate accuracy.

$$Acc = \frac{TP + TN}{TP + TN + FP + TN} \quad (27)$$

where *TP, TN, FP* and *FN* denote true positives, true negatives, false positives, and false negatives, respectively.

Pre quantifies the accuracy of positive predictions and is computed as:

$$Pre = \frac{TP}{TP + TN} \tag{28}$$

F1 balances Pre and RC, defined as

$$F1 = \frac{2\,Pre.RC}{Pre + RC} \tag{29}$$

where RC, also known as sensitivity, represents the fraction of *TP* cases properly detected by the model and is given as

$$RC = \frac{TP}{TP + FN} \tag{30}$$

The formula of JI can be expressed as

$$\text{JI} = \frac{\sum_{i=1}^{C} A_i \cap B_i}{\sum_{i=1}^{C} A_i \cup B_i} \tag{31}$$

A_i represents the number of pixels categorised into the i^{th} class, B_i denotes the number of pixels in the i^{th} class in the GT image, and C represents the overall number of clusters. The JI emphasises the agreement of overlapping areas in segmentation masks. These measurements provide vital insights into the performance and quality of image-processing algorithms, allowing academics and practitioners to evaluate the efficiency of different comparison methods. Higher pixel Acc, Pre, F1, and JI values imply better algorithm performance and segmentation outcomes.

EXPERIMENTAL RESULT

To further illustrate the variety of images from numerous standard datasets to demonstrate the approached method's robust anti-noise capabilities and excellent segmentation performance. These datasets include brain tumor images from Kaggle (https://www.kaggle.com/datasets/navoneel/brain-mri-images-for-brain-tumor-detection), chest CT scan images (https://www.kaggle.com/datasets/mohamedhanyyy/chest-ctscan-images), authorised medical datasets of brain tumors (https://www.med.upenn.edu/cbica/brats2020/data.html), and synthetic images from open web sources. These distinct images are exposed to varying noise levels and tested to validate the suggested algorithm's performance. The testing results for analysing the noise images were clarified with parameter measurement tables for

Table 2. Comparison of image denoising methods under various noise types and evaluation metric

Noise	Index	FCM	FCMKL	PFCM	KFPKL	KSSFKL
Gaussian (0, 0.7)	PSNR	10.5304	10.5310	10.5310	**10.5311**	10.5003
	Acc	**0.9070**	0.8018	0.7620	0.8303	0.9011
	Pre	0.9088	**0.9107**	**0.9107**	**0.9107**	0.8360
	F1	**0.9079**	0.8528	0.8298	0.8687	0.8673
	JI	0.8654	0.4498	0.3746	0.5254	**0.9390**
S & P (5%)	PSNR	6.6477	**6.6733**	6.6420	6.6501	6.6178
	Acc	0.3385	0.5936	0.5817	**0.7377**	0.7268
	Pre	**0.7727**	0.7604	0.7614	0.7288	0.6331
	F1	0.4708	0.6667	0.6595	**0.7332**	0.6768
	JI	0.3240	0.4961	0.4847	0.5282	**0.6280**
Impulse (15)	PSNR	**4.5244**	4.4451	4.4111	4.4562	4.4452
	Acc	0.1815	0.2211	0.2349	0.2753	**0.2774**
	Pre	0.2750	0.2733	0.2769	0.2321	**0.2777**
	F1	0.2194	0.2444	0.2205	**0.2518**	0.2413
	JI	0.8828	0.9234	0.9144	**0.9229**	0.9180
Speckle (0.5)	PSNR	**5.9101**	5.8744	5.8744	5.8975	5.8431
	Acc	0.6145	0.5834	0.6949	0.7251	**0.7284**
	Pre	**0.7394**	**0.7394**	0.7386	0.7351	0.5564
	F1	0.6712	0.6522	0.7160	0.7301	**0.9329**
	JI	0.6761	0.6255	0.8517	0.8722	**0.9329**
Rician (30)	PSNR	6.6587	6.6269	6.6587	6.6354	**6.7245**
	Acc	0.7808	0.7825	0.7808	0.7828	**0.7845**
	Pre	0.7678	0.6124	**0.7678**	0.6255	0.7296
	F1	0.7742	0.6871	0.7742	**0.7928**	0.7845
	JI	0.9236	0.8154	0.9236	0.8154	**0.9378**

different noise levels. Experimental data indicate that the proposed method gets a good result analysis of the parameter evaluation.

Testing and analysis of images

To ensure that this suggested approach is comparable to other algorithms such as FCM, FCMKL, PFCM, and KFPKL. Figure 2 shows that the result of the performance of algorithms that present different noises during the segmentation extraction successfully exhibits smaller inhomogeneity and indicates superior segmentation performance and robustness. The denoising process is applied to various noise types in the original image (OI). Each row corresponding to different noise applies the level range of Gaussian noise (normalized variance of 0.7), salt and pepper noise (intensity of 0.4), impulse noise (rate of 0.5), speckle noise (normalized variance of 0.5), and Rician noise (standard deviation of 30). Then, noise reduction would be applied using Gaussian blur. This noise level enables a clear comparison of each algorithm, implying denoising performance under specific noise conditions. This assessment measures PSNR, accuracy, precision, F1 score, and Jaccard index on synthetic datasets.

Furthermore, the segmentation results are presented in Table 2, which crossovers the different segmentation results compared to the GT image. The bold values indicate the outperformance of other denoising techniques. Although these values, due to running time, create random variability, the more consistent yielding better segmentation results trend of this proposed method than various algorithms are significant. Our methodology: This technique is typically appropriate and attains greater segmentation accuracy, improving noise reduction and overall image clarity.

Figures 3-7 present bar graphs comparing the performance of various algorithms under different noise levels. These graphs are present in Figure 2, which illustrates the metrics evaluated across various noise intensities at the level of Gaussian; mean values of 0 and normalized variances

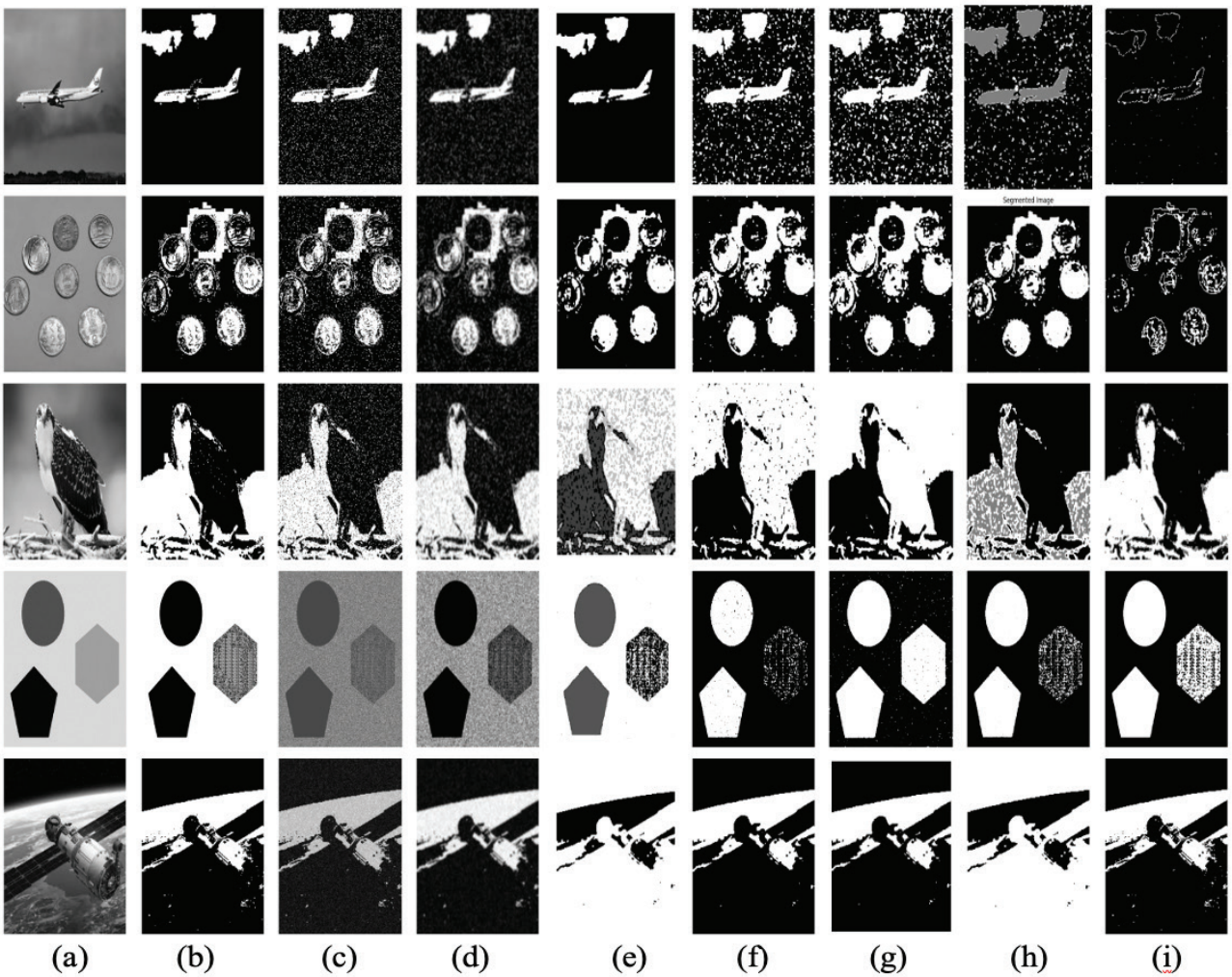

Figure 2. (a) OI; (b) Ground Truth; (c) Noise Image; (d) Denoise image; (e) FCM; (f) FCMKL; (g) PFCM; (h) KFPKL; (i) Proposed (KSSFKL).

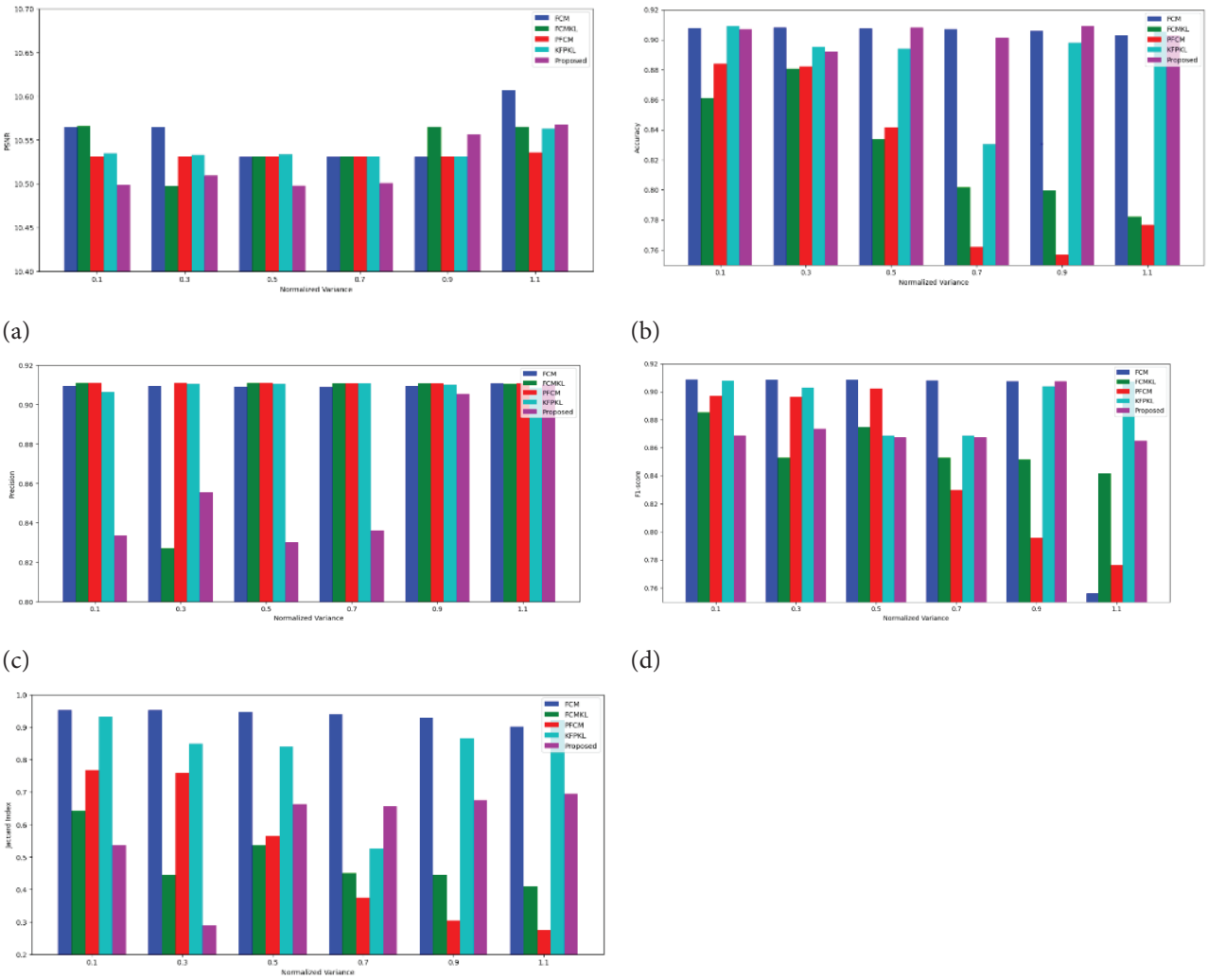

Figure 3. Figure 2 shows the performance curves of multiple techniques applied to the first-row image affected by Gaussian noise. a) PSNR; b) Acc; c) Pre; d) F1; e) JI.

from 0.1 to 1.1 are considered. Salt and pepper noise is intensities from 1% to 6%. Impulse noise is applied at a rate ranging from 5% to 30%. Speckle noise shows normalized variances from 0.1 to 1.1, and Rician noise has standard deviations increasing from 10 to 60. It is easy to handle. It is one of the statistical methods randomly added to the image function to generate this noise.

Medical Image Segmentation

Evaluating the method on both synthetic and real datasets ensures robustness, as synthetic data helps test theoretical aspects of the model, while real data validates its practical effectiveness in real-world scenarios like brain MRI or lung CT scans. Synthetic data are crucial in this interplay since they can provide large and diverse data. However, privacy is an important factor which is not guaranteed by data fidelity. To this end, best practices should be adopted for data protection, clearer standards for assessing identifiability, and proportionate regulatory approaches to facilitate innovation while ensuring privacy. Consequently, the accessibility of superior synthetic data can facilitate researchers in the development of multimodal AI models. Furthermore, synthetic data can enable the simulation of complex patient scenarios that might not be frequently encountered in real datasets, thereby enhancing the robustness of healthcare systems against rare but critical conditions. Moreover, by utilizing synthetic data, researchers can bypass many logistical and ethical hurdles that occur during the aggregation and analysis of multimodal data, thus accelerating the pace of research. Ultimately, the use of medical data can significantly advance personalised medicine, improving

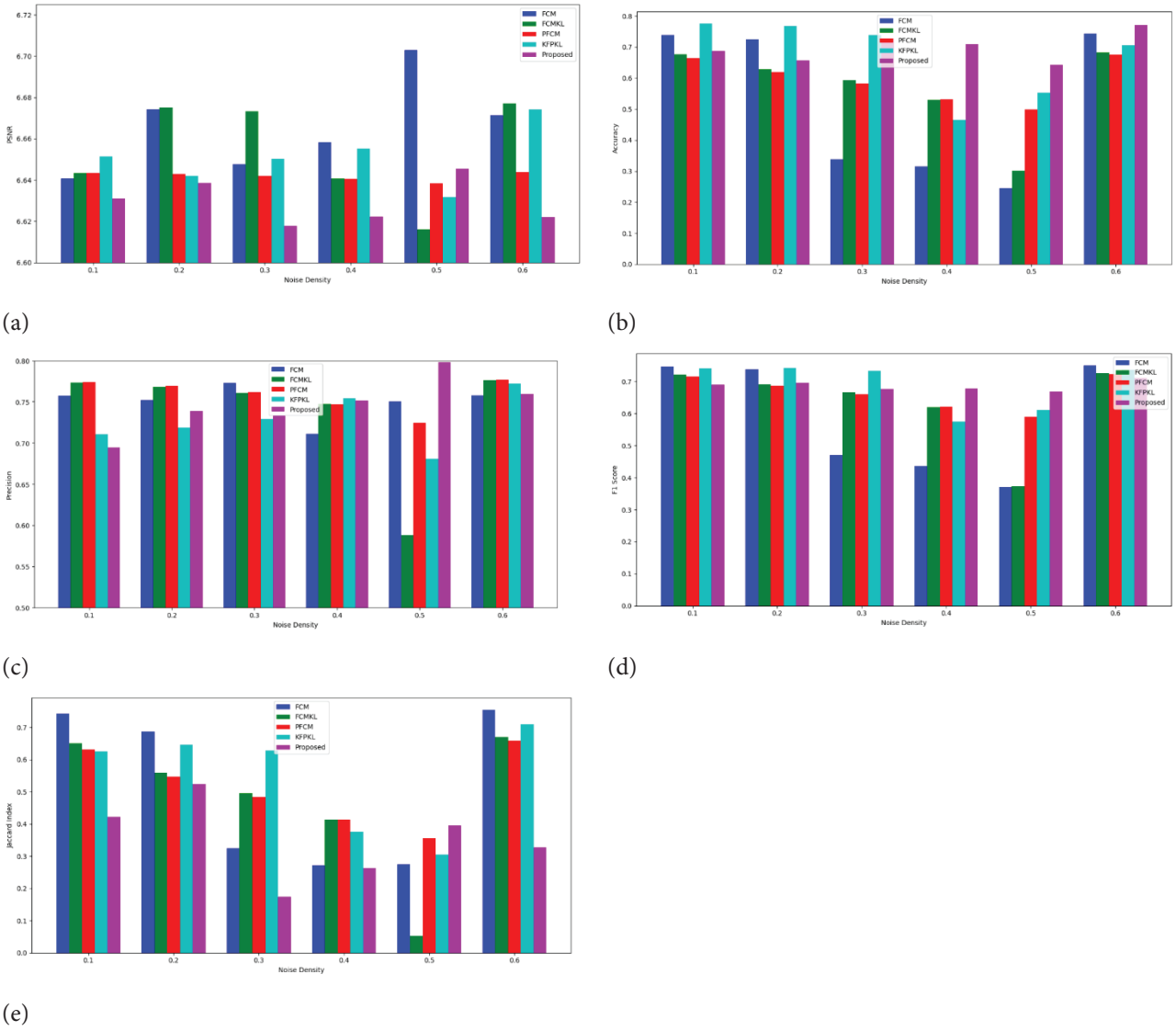

Figure 4. Figure 2 shows the performance curves of multiple techniques applied to the second-row image affected by salt noise. a) PSNR; b) Acc; c) Pre; d) F1; e) JI.

treatment efficacy and patient outcomes while upholding stringent data privacy standards. Now, we discuss the medical image segmentation of Brain MRI images and lung CT scan images. Image segmentation was formulated to segment different tissue types: WM, GM, and CSF—additionally, the Gaussian noise level range at 0.7 and salt and pepper noise (0.4). Then, denoise techniques applying Gaussian blur detail segmentation results are shown in Figure 8, which implies the FCM, FCMKL, PFCM, KFPKL, and proposed method. KSSFKL, better than other methods, reduces noise reduction through kernel approach and KL-divergence, which allows the clustering process to focus on relevant image features while suppressing the influence of noise. This results in more stable and accurate segmentation, especially in medical image analysis, where noise can obscure critical details. Each clustering method resulted in the segmentation of different noise types; the extraction result is shown in Figure 9. We get more accurate segmentation results compared to other cluster techniques to evaluate the similarity measurement compared to the GT image to existing output image to draw the bar graph presented in Figure 10 of accurate performance in MRI and CT scan images.

Visualize the Approach Method of Brats2020 without Noise

The Brats2020 dataset, known for its diverse and challenging brain tumor cases, was employed to test rigorously. Figure 11 illustrates the range defined by the parameter rho (ρ)= 5,10,15 and lambda (λ)= 5,10,15 with the call as

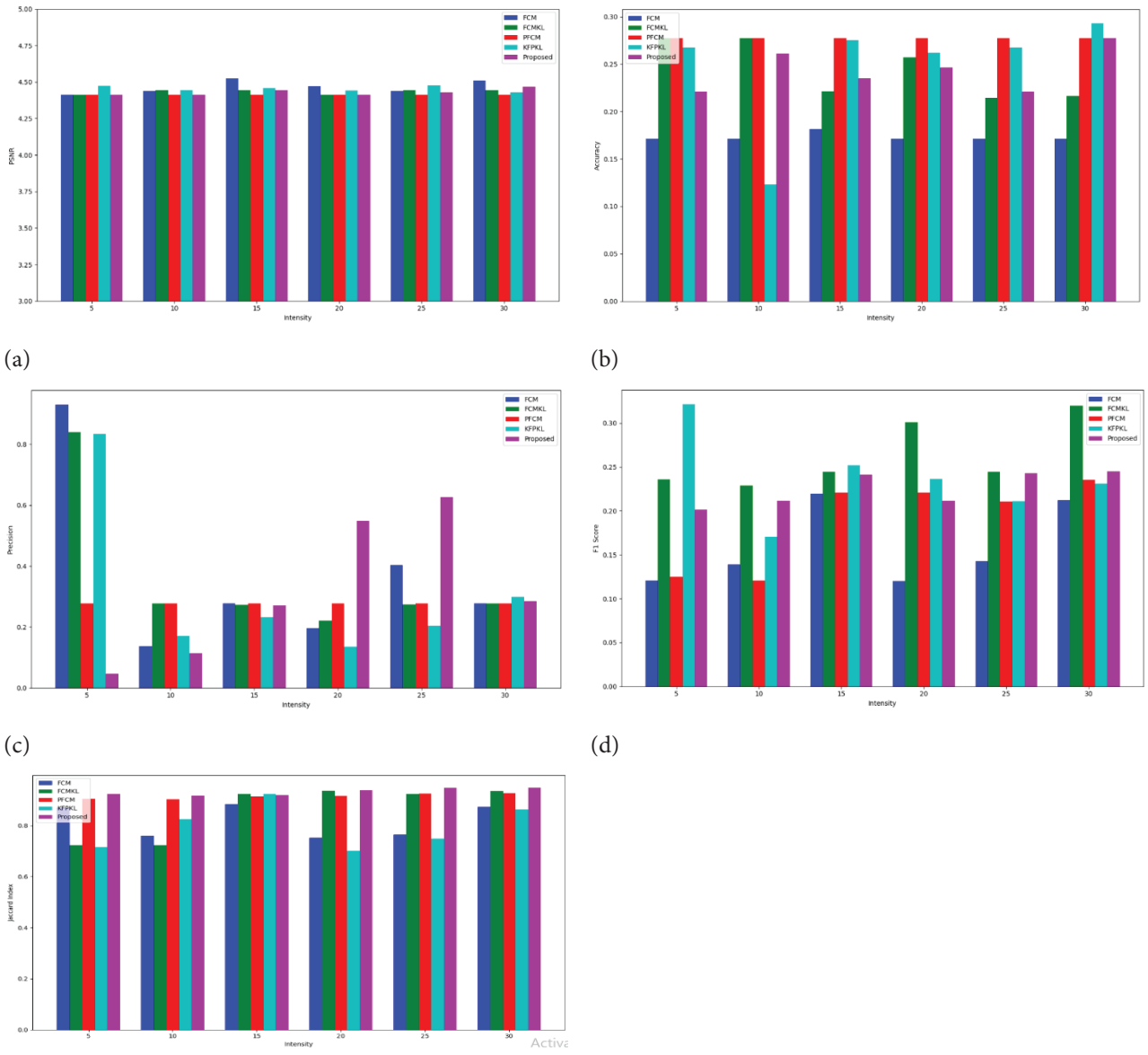

Figure 5. Figure 2 shows the performance curves of various algorithms for the third-row image that has been contaminated by impulse noise. a) PSNR; b) Acc; c) Pre; d) F1; e) JI.

various segmentation approaches to test different cluster configurations. It performs the KSSFKL for each combination of parameter values. The parameter values affect overall clustering performance. Different datasets may require different data balance parameters. Sometimes, the performance level exists.

Our proposed method obtained good segmentation and accurate segmentation results. Aggregating the noise pixels of an image produces more accurate clustering by distinguishing relevant features from noise. The proposed method shows that the optimization algorithm can obtain better detection results when processing noise images.

RESULTS AND DISCUSSION

In our research, we employed a blend of synthetic and authentic datasets to validate the robustness of our suggested model. Synthetic data enabled us to systematically evaluate theoretical components, offering a controlled setting for replicating intricate patient scenarios that are infrequent in actual datasets yet crucial to examine. The system enabled the simulation of various abnormal conditions,

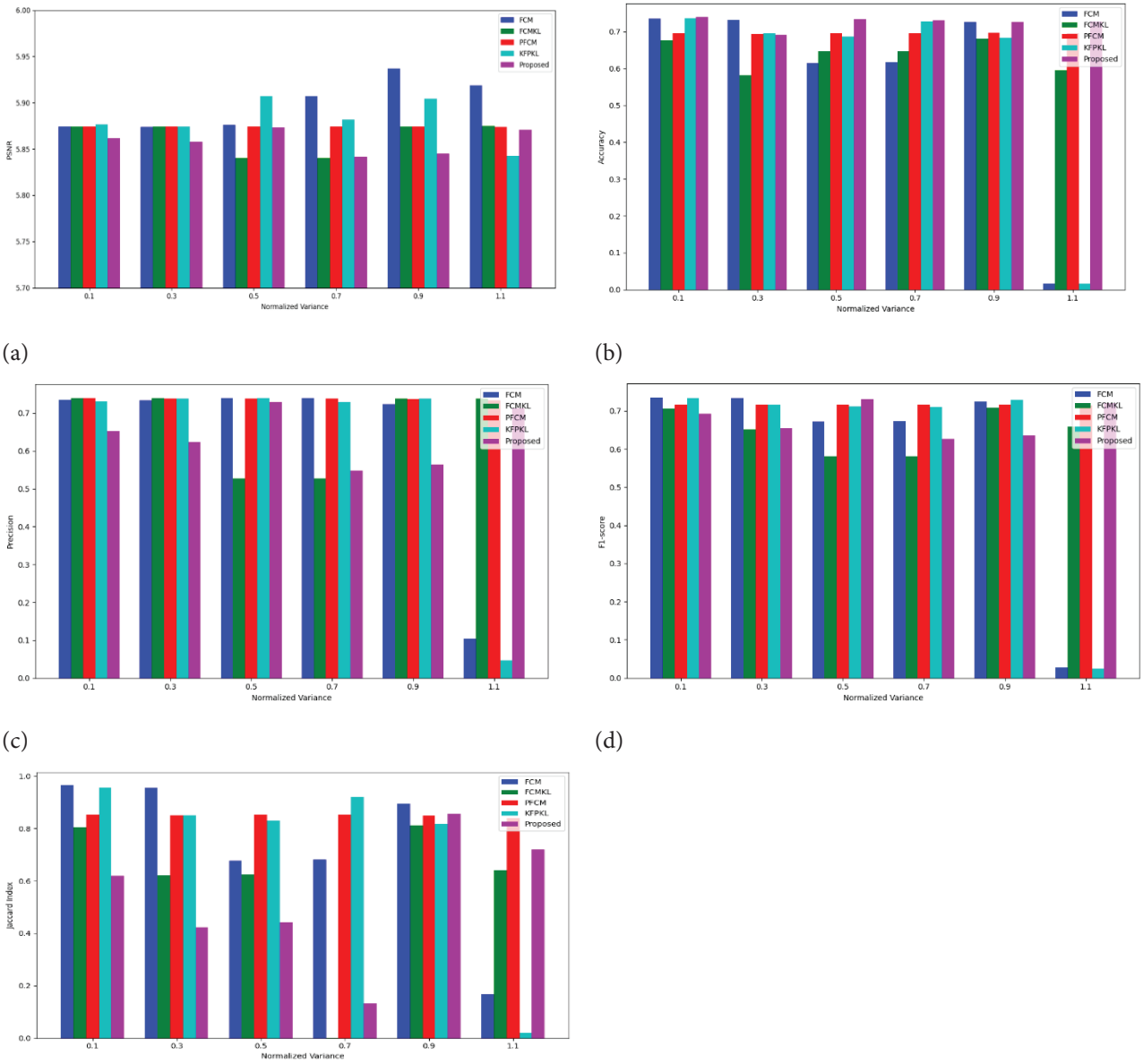

Figure 6. Figure 2 shows the performance curves of various algorithms for the fourth-row image contaminated by speckle noise. a) PSNR; b) Acc; c) Pre; d) F1; e) JI.

improving the model's adaptability to various healthcare challenges such as brain MRI and lung CT scan analysis. Meanwhile, real data confirmed the practical performance of our model in real-world applications, ensuring that it is highly applicable to real clinical situations. Our analysis showed that many current methods are unable to effectively reduce noise interference. In contrast, our proposed KSSFKL method significantly reduces noise's impact, achieving more accurate segmentation results. For subjective analysis, the clustering effect generated by our method was beneficial for analysing tumor shape, size, and texture. By implementing morphological reconstruction, we can define precise edges and boundaries, enabling a more accurate and detailed segmentation of internal regions without ambiguity. Following this, our objective analysis further demonstrated the benefits of our approach. As seen in Table 3, our methods outperformed more advanced techniques. This performance was achieved within a short processing time, raising the potential of this method as a reliable and time-efficient solution for real-world medical imaging applications.

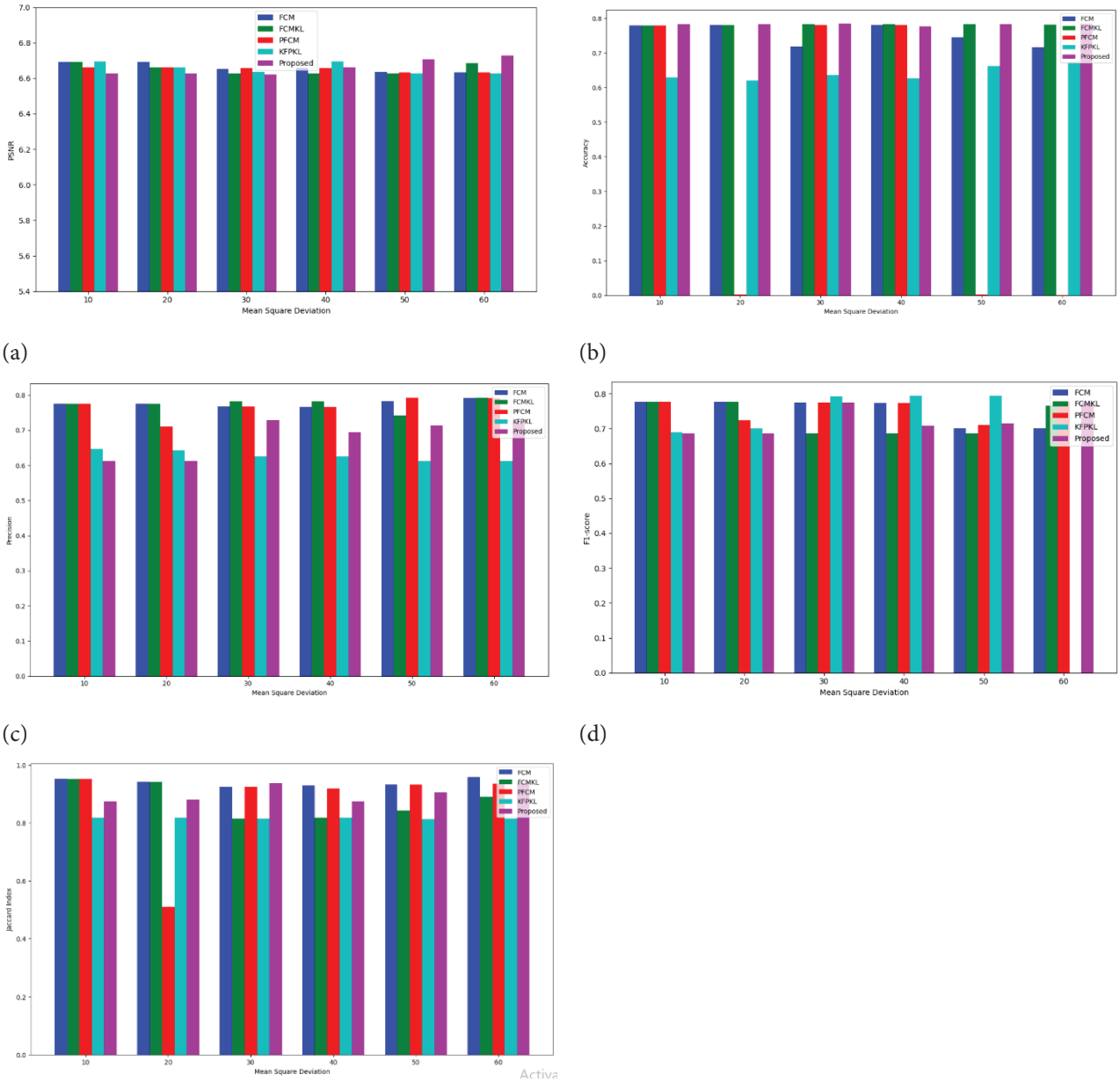

Figure 7. Figure 2 shows the performance curves of various algorithms for the fifth-row image that has been contaminated by rician noise. a) PSNR; b) Acc; c) Pre; d) F1; e) JI.

Table 3. The statement contrasts the runtimes of several clustering techniques, highlighting the computational efficiency of each

Clustering methods	Running time (s)
FCM	0.7 min
FCMKL	1.2 min
PFCM	2 min
KFPKL	4.9 min
KSSFKL	2.8 min

CONCLUSION

This study introduces a kernel-based semi-supervised fuzzy clustering method that integrates Kullback–Leibler divergence to tackle common image clustering problems such as noise, uncertainty, and non-linear patterns. A Gaussian kernel is used to better manage noise and complex structures within the semi-supervised fuzzy clustering framework. An extensive evaluation across multiple datasets, including computed tomography scans, brain magnetic resonance imaging data, the BraTS2020 Dataset, and synthetic

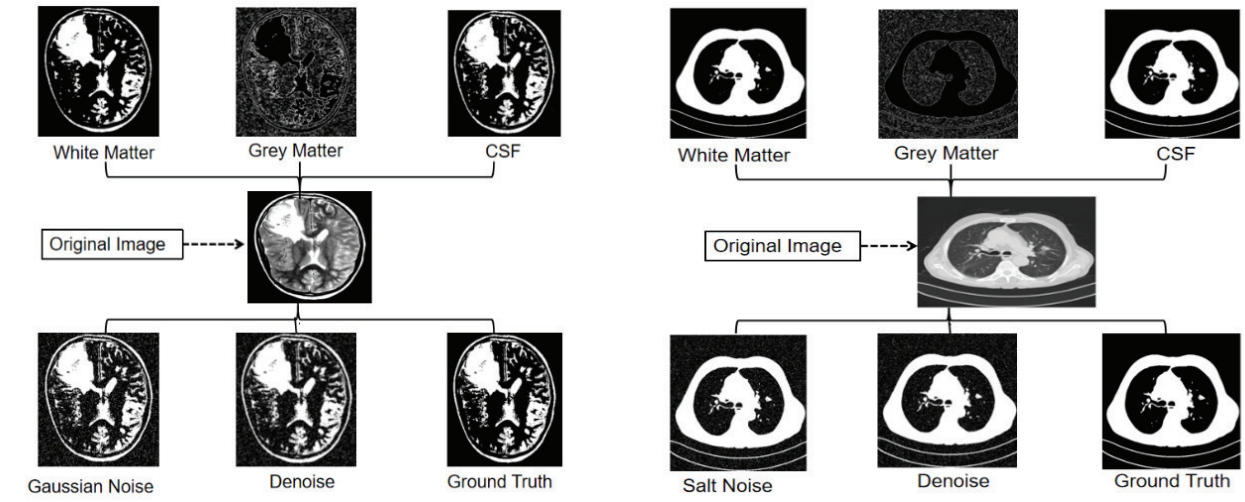

(a) (b)

Figure 8. a) represent the Brain MRI image and b) represent the lung CT scan image.

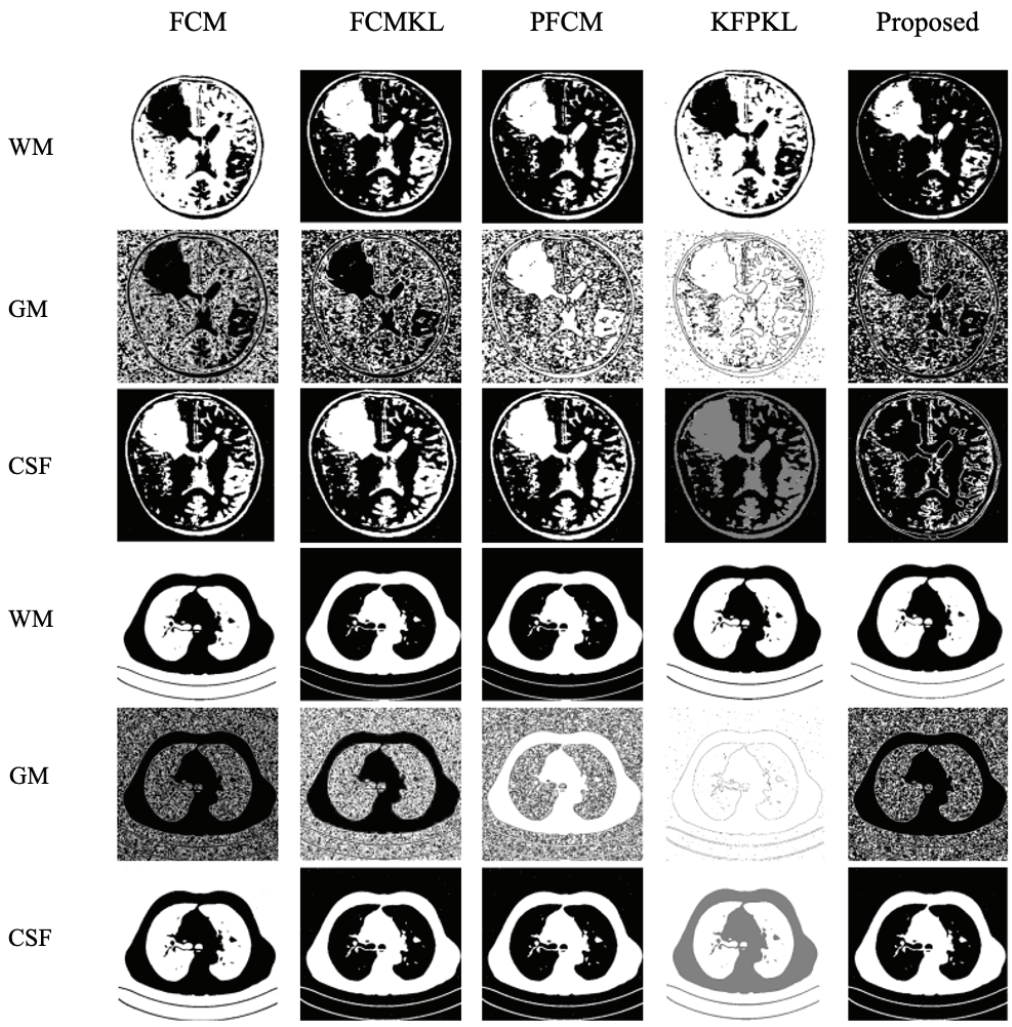

Figure 9. Comparison of segmentation results using different clustering algorithms. The columns correspond to segmentation results obtained using FCM, FCMKL, PFCM, KFPKL, and the proposed method. Rows denote the segmentation of WM, GM, and CSF.

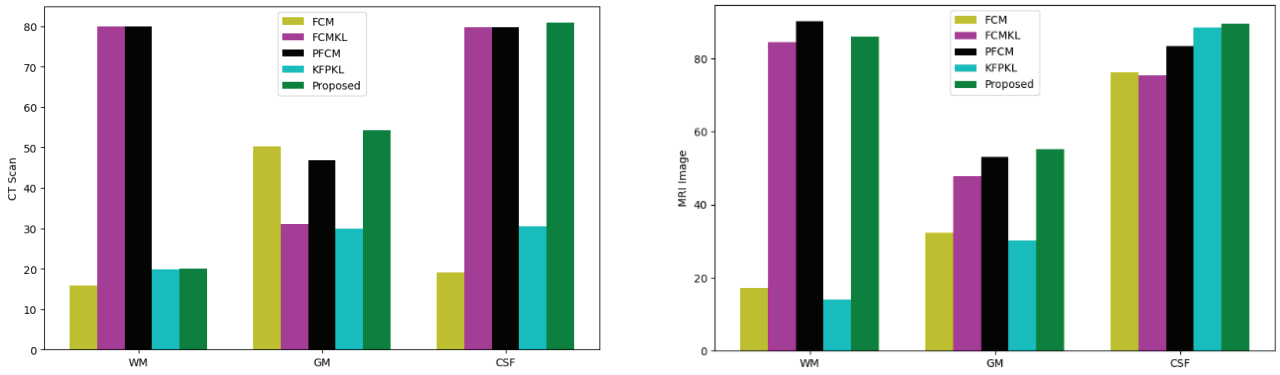

(a) (b)

Figure 10. (a) and (b) denote the precision of the CT scan and MRI imaging efficacy.

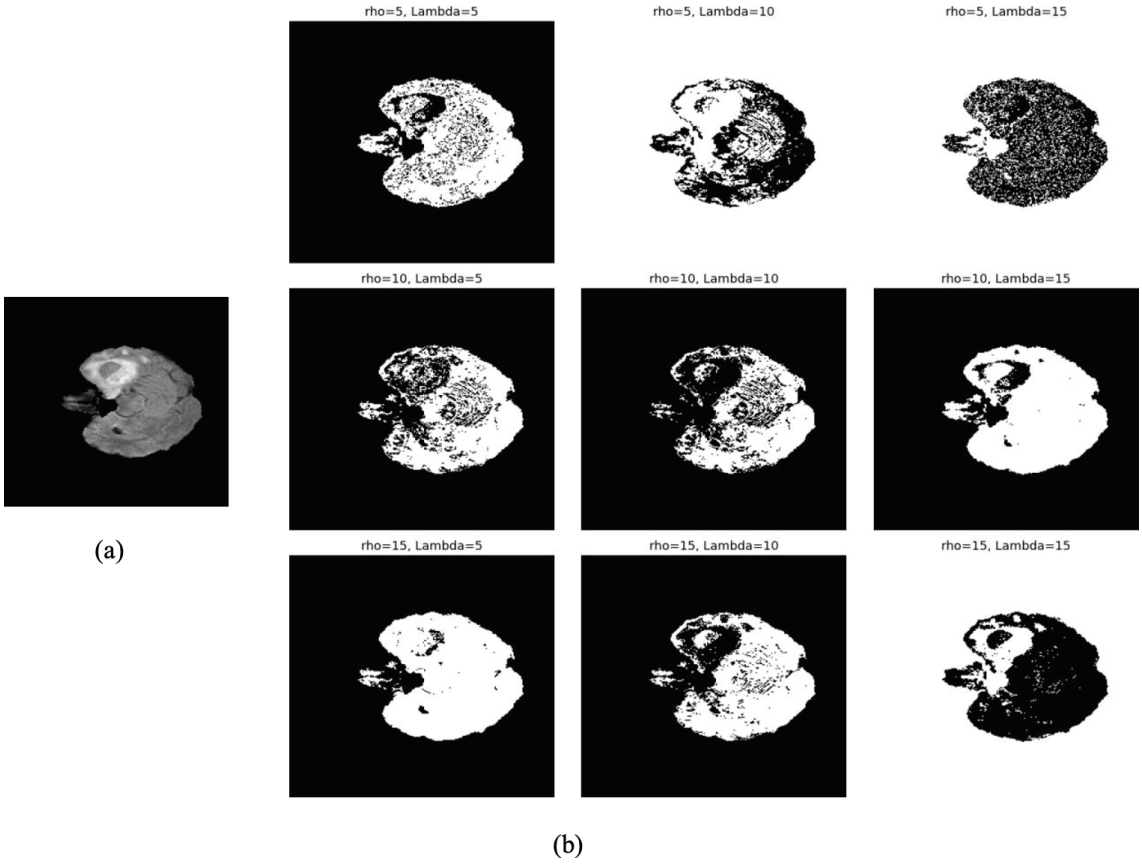

Figure 11. Result of KSSFKL applying different rho and lambda values.

images, unequivocally demonstrates the efficacy of our strategy. The segmentation accuracy has significantly improved compared to current state-of-the-art methods. Both subjective and objective evaluations confirm the advantages of clustering precision, artefact reduction, convergence efficiency, and computational speed. Comparative results show that the proposed method is also faster than several existing approaches, which supports its practical use. Overall, the method improves image segmentation by strengthening feature representation and improving clustering quality. Future work will focus on automatically estimating the number of clusters and incorporating more image-specific prior knowledge. It is crucial to acknowledge that each algorithm is constrained to 1000 iterations. The potential applications of our

approach extend beyond medical imaging. Its noise resistance renders it advantageous for several applications requiring precise segmentation, including remote sensing, satellite imagery, and industrial inspection, where uncertainty and noise present inherent challenges.

AUTHORSHIP CONTRIBUTIONS

Muthulakshmi K: Methodology, conceptualization, Formal analysis, Writing Original draft preparation, and editing. Jayalakshmi M: Supervision, conceptualization, Editing and Validation.

DATA AVAILABILITY STATEMENT

The authors confirm that the data that supports the findings of this study are available within the article. Raw data that support the finding of this study are available from the corresponding author, upon reasonable request.

CONFLICT OF INTEREST

The author declared no potential conflicts of interest with respect to the research, authorship, and/or publication of this article.

ETHICS

There are no ethical issues with the publication of this manuscript.

STATEMENT ON THE USE OF ARTIFICIAL INTELLIGENCE

Artificial intelligence was not used in the preparation of the article.

REFERENCES

[1] Pedrycz W, Waletzky J. Fuzzy clustering with partial supervision. IEEE Trans Syst Man Cybern B Cybern 1997;27:787–795. [CrossRef]

[2] Goyal S, Kumar S, Zaveri MA, Shukla AK. Fuzzy similarity measure based spectral clustering framework for noisy image segmentation. Int J Uncertain Fuzziness Knowl Based Syst 2017;25:649–673. [CrossRef]

[3] Du M, Ding S, Xue Y. A robust density peaks clustering algorithm using fuzzy neighborhood. Int J Mach Learn Cybern 2018;9:1131–1140. [CrossRef]

[4] Cuevas E, Fausto F, González A. Locust search algorithm applied to multi-threshold segmentation. In: New Advancements in Swarm Algorithms: Operators and Applications. 2020:211–240. [CrossRef]

[5] Oskouei AG, Samadi N, Tanha J. Feature-weight and cluster-weight learning in fuzzy c-means method for semi-supervised clustering. Appl Soft Comput 2024;161:111712. [CrossRef]

[6] Pan H, Liu W, Li L, Zhou G. A novel level set approach for image segmentation with landmark constraints. Optik 2019;182:257–268. [CrossRef]

[7] Atanassov K. Review and new results on intuitionistic fuzzy sets. Preprint IM-MFaIS-1-88, Soa 1988:1–8.

[8] Bora DJ, Gupta DA. A comparative study between fuzzy clustering algorithm and hard clustering algorithm. arXiv Prepr arXiv:1404.6059. 2014 Apr 24.

[9] Ferraro MB, Giordani P. Soft clustering. Wiley Interdiscip Rev Comput Stat 2020;12:e1480. [CrossRef]

[10] Pitchai R, Supraja P, Victoria AH, Madhavi MJ. Retracted article: Brain tumor segmentation using deep learning and fuzzy k-means clustering for magnetic resonance images. Neural Process Lett 2021;53:2519–2532. [CrossRef]

[11] Schölkopf B, Smola A, Müller KR. Kernel principal component analysis. In: Int Conf Artif Neural Netw 1997:583–588. [CrossRef]

[12] Kmita K, Kaczmarek-Majer K, Hryniewicz O. Explainable impact of partial supervision in semi-supervised fuzzy clustering. IEEE Trans Fuzzy Syst 2024 Feb 27. [CrossRef]

[13] Guo Y, Sengur A. A novel color image segmentation approach based on neutrosophic set and modified fuzzy c-means. Circuits Syst Signal Process 2013;32:1699–1723. [CrossRef]

[14] Miyamoto S, Ichihashi H, Honda K. Algorithms for fuzzy clustering. Heidelberg: Springer; 2008.

[15] Klir G, Yuan B. Fuzzy sets and fuzzy logic. New Jersey: Prentice Hall; 1995. [CrossRef]

[16] Zadeh LA. Fuzzy sets. University of California Electronic Research Laboratory. California: University of California;1965. [CrossRef]

[17] Zhao F, Yang Y, Liu H, Wang C. A robust multi-view knowledge transfer-based rough fuzzy c-means clustering algorithm. Complex Intell Syst 2024 Apr 25:1–28.

[18] Dattoli G, Ricci PE, Cesarano C. The Lagrange polynomials, the associated generalizations, and the umbral calculus. Integral Transf Spec Funct 2003;14:181–186. [CrossRef]

[19] Graves D, Pedrycz W. Kernel-based fuzzy clustering and fuzzy clustering: A comparative experimental study. Fuzzy Sets Syst 2010;161:522–543. [CrossRef]

[20] Zhu H, Xie W, Mu Y, Xu J, Wang FL, Qu Y, et al. A new semi-supervised fuzzy k-means clustering method with dynamic adjustment and label discrimination. Neural Comput Appl 2024;36:4709–4725. [CrossRef]

[21] Lavanya KG, Dhanalakshmi P, Nandhini M. A novel enhancement-based rapid kernel-induced intuitionistic fuzzy c-means clustering for brain tumor image. Soft Comput 2024;28:6657–6670. [CrossRef]

[22] Cuong BC, Kreinovich V. Picture fuzzy sets. J Comput Sci Cybern 2014;30:409–420.

[23] Wu C, Chen Y. Adaptive entropy weighted picture fuzzy clustering algorithm with spatial information for image segmentation. Appl Soft Comput 2020;86:105888. [CrossRef]
[24] Wu C, Zhang J. Robust semi-supervised spatial picture fuzzy clustering with local membership and KL-divergence for image segmentation. Int J Mach Learn Cybern 2022;13:963–987. [CrossRef]
[25] Shlens J. Notes on Kullback-Leibler divergence and likelihood. arXiv Prepr arXiv:1404.2000. 2014 Apr 8.
[26] Gharieb RR, Gendy G. Fuzzy c-means with local membership based weighted pixel distance and KL divergence for image segmentation. J Pattern Recognit Res 2015;10:53–60. [CrossRef]
[27] Halder A, Talukdar NA. Kernel induced semi-supervised spatial clustering: A novel brain MRI segmentation technique. Multimed Tools Appl 2024;83:49213–49241. [CrossRef]
[28] Thong PH, Son LH. Picture fuzzy clustering: A new computational intelligence method. Soft Comput 2016;20:3549–3562. [CrossRef]
[29] Cristianini N. An introduction to support vector machines and other kernel-based learning methods. Cambridge: Cambridge Univ Press; 2000. [CrossRef]
[30] Liu Q, Lu H, Ma S. Improving kernel Fisher discriminant analysis for face recognition. IEEE Trans Circuits Syst Video Technol 2004;14:42–49. [CrossRef]
[31] Antolìn AG, Garcìa JP, Gòmez JL. Radial basis function networks and their application in communication systems. In: Comput Intell Eng Manuf 2007:109–130. [CrossRef]
[32] Taha K. Semi-supervised and un-supervised clustering: A review and experimental evaluation. Inf Syst 2023;114:102178. [CrossRef]
[33] Khatri I, Kumar D, Gupta A. A noise robust kernel fuzzy clustering based on picture fuzzy sets and KL divergence measure for MRI image segmentation. Appl Intell 2023;53:16487–16518. [CrossRef]
[34] Kumar SA, Harish BS, Aradhya VM. A picture fuzzy clustering approach for brain tumor segmentation. In: Int Conf Cogn Comput Inf Process 2016:1–6. [CrossRef]
[35] Chen DZ. Fuzzy clustering using kernel method. IEEE, Nanjing, China. 2002.

APPENDIX

The derivation method for equations (25–26) in the suggested algorithm is as follows. KL divergence clustering is used in the resilient semi-supervised fuzzy clustering optimization model.

$$J = \sum_{j=1}^{N}\sum_{\mathrm{i}=1}^{C} u_{ij}^{m} d_{ij}^{2} + \rho \sum_{j=1}^{N}\sum_{\mathrm{i}=1}^{C} \left(u_{ij} - f_{ij} b_i\right)^{m} d_{ij}^{2} + \lambda \sum_{j=1}^{N}\sum_{\mathrm{i}=1}^{C} \left(u_{ij}\left(\log u_{ij}\right)\right) \tag{32}$$

Where,

$$\begin{aligned} d^2 &= \left\|\phi(y_i) - \phi(y_j)\right\|^2 \\ &= \left\|\phi(y_i) - \phi(y_j)\right\|^T \left\|\phi(y_i) - \phi(y_j)\right\|^2 \\ &= \phi(y_i)^T\phi(y_i) - \phi(y_i)^T\phi\left(y_j\right) - \phi\left(y_j\right)^T\phi(y_i) + \phi\left(y_j\right)^T\phi\left(y_j\right) \\ &= \phi(y_i)^T\phi(y_i) + \phi\left(y_j\right)^T\phi\left(y_j\right) - 2\phi(y_i)^T\phi(y_j) \end{aligned}$$

The mapping utilized for the transformation of samples to higher dimensional space is represented by ϕ. The optimization problem equation (16) for the RBF kernel function using equation (17) can be rewritten as

$$\begin{aligned} d^2 &= k(y_i, y_i) + k\left(y_j, y_j\right) - 2k\left(y_i, y_j\right) \\ &= 2 - 2k\left(y_i, y_j\right) = 2\left(1 - k\left(y_i, y_j\right)\right) \end{aligned}$$

To determine the partial derivatives of $\lambda, u = 0$, by using equation (24):

$$\frac{\partial J}{\partial \lambda} = \sum_{j=1}^{N}\sum_{\mathrm{i}=1}^{C} \left(u_{ij}(\log u_{ij})\right) = 0 \tag{33}$$

$$\begin{aligned} \frac{\partial J}{\partial u_{ij}} = &\sum_{j=1}^{N}\sum_{\mathrm{i}=1}^{C} m\, u_{ij}^{m-1}\left(1 - k(y_i, y_j)\right) + \rho \sum_{j=1}^{N}\sum_{\mathrm{i}=1}^{C} m\left(u_{ij} - f_{ij} b_i\right)^{m-1}\left(1 - k(y_i, y_j)\right) \\ &+ \lambda \sum_{j=1}^{N}\sum_{\mathrm{i}=1}^{C}\left(1 + \log u_{ij}\right) = 0 \end{aligned} \tag{34}$$

Simplify the equation (34), we obtained u_{ij}:

$$2u_{ij}\left(1 - k\left(y_i, y_j\right)\right) + 2\rho\left(u_{ij} - f_{ij} b_i\right)\left(1 - k\left(y_i, y_j\right)\right) + \lambda + \lambda \log u_{ij} = 0.$$

Derive the above equation to get the derivation of

$$u_{ij} = \frac{1}{1+\rho}\left[-\frac{\lambda - \lambda \log u_{ij}}{2\left(1 - k\left(y_i, y_j\right)\right)} + \rho f_{ij} b_i\right]$$

and then,

$$\log u_{ij} = \frac{-\lambda + 2(1+\rho)\left(1 - k\left(y_i, y_j\right)\right)[\rho f_{ij} b_i - u_{ij}]}{\lambda}$$

$$u_{ij} = e^{\frac{-\lambda + 2(1+\rho)\left(1 - k\left(y_i, y_j\right)\right)[\rho f_{ij} b_i - u_{ij}]}{\lambda}}$$

Furthermore, obtain

$$u_{ij} = \frac{\exp\left(\dfrac{-\lambda + 2(1+\rho)(1 - k\left(y_j, v_i\right)[\rho \sum_{\mathrm{i}=1}^{C} f_{ij} b_j - u_{ij}]}{\lambda}\right)}{\sum_{k=1}^{C} \exp\left(\dfrac{-\lambda + 2(1+\rho)(1 - k\left(y_j, v_k\right)[\rho \sum_{\mathrm{i}=1}^{C} f_{ij} b_j - u_{ij}]}{\lambda}\right)} \tag{35}$$

and

$$v_i = \frac{\sum_{j=1}^{N} u_{ij} k\left(y_j, v_i\right) y_j + \rho \sum_{j=1}^{N}\left(u_{ij} - f_{ij} b_i\right)^2 y_j}{\sum_{j=1}^{N} u_{ij} k\left(y_j, v_i\right) y_j + \rho \sum_{j=1}^{N}\left(u_{ij} - f_{ij} b_i\right)^2} \tag{36}$$

Finally, using these equations, we obtained the membership value u_{ij} and the cluster center v_i for the proposed image segmentation approach.